Zeitschrift für Physikalische Chemie, **215**, 6, 811–824 (2001)

Shock Tube Study on the Reaction of Si Atoms with CH_3 with Respect to SiC Formation

By A. Kunz, K. A. Bhaskaran and R. Roth*

Institut für Verbrennung und Gasdynamik, Gerhard-Mercator-Universität Duisburg,
D-47048 Duisburg, Germany

Dedicated to Prof. Dr. Dr. h.c. mult. Jürgen Troe
on the occasion of his 60th birthday

(Received July 11, 2000; accepted September 8, 2000)

Shock Tube / Chemical Kinetics / Rate Coefficient / Silicon / Methyl Radical / SiC

The reaction kinetics of ground state Si atoms was studied behind reflected shock waves in the presence of excess CH_4 and CH_3, respectively. The very fast Si atom formation by the thermal decomposition of SiH_4 and Si_2H_6 was used as a reliable Si atom source at temperatures $T > 1550\,K$. CH_3 was formed by the thermal decomposition of different source gases like CH_3Cl and CH_3I. All test gases were highly diluted in argon. The atomic resonance absorption spectroscopy (ARAS) was applied for time-resolved measurements of Si and H atoms and it was found that the reaction of Si atoms with CH_4 (R1) is much slower than the reaction of Si atoms with CH_3 (R2) which seems to be an important reaction leading to the formation of very reactive intermediate species on its way to form SiC. The product channels are discussed and a temperature independent mean rate coefficient for (R2) was determined:

$$Si + CH_3 \overset{k_{2a}}{\rightleftharpoons} SiCH + H_2 \tag{R2a}$$

$$\overset{k_{2b}}{\rightleftharpoons} SiCH_2 + H \tag{R2b}$$

with $k_{2b}/k_{2a} < 0.1$ and a mean value for $k_2 = 2.0 \pm 0.69 \cdot 10^{14}\,cm^3\,mol^{-1}\,s^{-1}$. A reaction mechanism including the established GRI (Gas Research Institute) mechanism is presented which explains all measured Si and H concentration profiles obtained during this study.

Introduction

The significance of silicon carbide as one of the most important ceramics is well recognised as also the persisting interest in optimizing the proper-

---

* Corresponding author. E-mail: roth@ivg.uni-duisburg.de

ties of the final bulk material to meet highest demands. The production of silicon carbide nano-powder with characteristics like highest purity and quality, high specific surface area, and high sintering quality is therefore of great importance. The most established SiC production process is still the energy intensive Atcheson process [1], where SiO_2 reacts with carbon to form SiC and the resulting CO, which has to separated in a rather expensive process. Different ways of Chemical Vapour Deposition (CVD) processes are available for very high purity SiC thin film production. For SiC nano-powder production of highest purity the gas-phase synthesis in high-temperature reactors became the focus of interest during the last decade. A general overview of the synthesis of particles in high temperature gas-phase reactors is given by Wooldridge [2] and Pratsinis [3] has presented the flame aerosol processes. Many studies about different SiC synthesis routes were published in the last years. Such processes are partly combined with RF, microwave or laser energy inputs. Different source gases have been used like SiH_4/CH_4, SiH_4/C_2H_4, Si_2H_6/CH_4, $SiCl_4/CH_4$, CH_3SiCl_3, $(CH_3)_2SiHCl$, $(CH_3)_2SiCl_2$, $(CH_3)_4Si$, and $Si(CH_3)_2(C_2H_5O)_2$. To understand and to optimize such processes, reliable kinetic and thermodyamic data of important gas-phase reactions are necessary.

In many studies where silanes or chlorosilanes and methane are used as source gases, it is mentioned that with higher temperatures higher SiC yields can be obtained. Some of these workers have assumed homogeneous gas-phase reactions of gaseous silicon as the favoured reaction route to form SiC. In view of the higher stability of methane compared to those of the silanes, these deliberations are acceptable. Tamou *et al.* [4] have synthesized SiC powder from $SiCl_4/CH_4$ using H_2 as a quenching gas in a thermal plasma CVD reactor. According to equilibrium calculations they suggested that the reaction $Si(g) + CH_x$ $(x = 0...4)$ is responsible for the formation of SiC. Guo *et al.* [5] have synthesized SiC powder by introducing pure silicon powder into a carrier gas consisting of CH_4/Ar or CH_4 only, which is injected into an induction plasma in hot and cold wall reactors, respectively. They also strongly suggested the reaction of gaseous silicon with decomposition products of methane as the predominant mechanism for SiC formation.

A comprehensive study of the reaction of Si atoms with several hydrocarbons was performed by Basu and Husain [6, 7]. They have studied reactions of ground state Si atoms with different acetylenes and olefins (e.g. C_2H_2, C_2H_4, C_3H_6, C_4H_8) in a slow-flow reactor at room temperature. Si atoms were generated by pulsed irradiation of $SiCl_4$ and an atomic resonance absorption system was used for the Si detection. Differences between the absorption decay caused by the reaction of Si with $SiCl_4$ [8, 9] and a faster decay obtained when acetylenes and olefins are added were analysed and reported in form of rate coefficients. They have also studied the reaction of Si with CH_4 [10] and reported an upper limit for the rate coefficient at room temperature to be $k_1 \leq 6.0 \cdot 10^9\ \mathrm{cm^3\,mol^{-1}\,s^{-1}}$ which was much slower compared to reactions with olefines or acetylenes which have rate coefficient values almost equal to the collision frequency.

In this study the formation and consumption of silicon atom concentrations by added CH_4 and CH_3 at high temperatures was measured behind reflected shock waves. An ultra-high vacuum(UHV)-shock tube reactor equipped with highly sensitive atomic resonance absorption spectroscopy (ARAS) is used to detect time resolved Si- and H-atom concentrations in highly diluted $SiH_4/Si_2H_6/CH_4/CH_3Cl/CH_3I/Ar$ mixtures. The paper describes the experimental technique and discusses the kinetic results based on a reaction model, which can predict all measured signals over a wide range of mixtures compositions and temperatures.

Experimental

The experiments were carried out behind reflected shock waves in a stainless steel shock tube of 80 mm internal diameter. The driver section was 3.5 m, the driven section 6.0 m in length, which was specially prepared for ultra-high-vacuum (UHV) requirements. The driven section can be baked out and pumped down to pressures below $2 \cdot 10^{-8}$ mbar by a turbo molecular pump. The gas mixtures used were prepared manometrically in a stainless steel UHV cylinder which can be pumped down by the combination of a chemical diaphragm pump and a turbo-molecular drag pump. The leak and/or outgassing rate was in the order of $(1 \pm 0.5) \times 10^{-7}\ \mathrm{mbar\,s^{-1}}$ for both driven section and vessel. The gases and liquids used were of highest commercial purity: Ar $\geq$ 99.9999%, $Si_2H_6 \geq 99.9\%$, $SiH_4 \geq 99.999\%$, $CH_3Cl \geq 99.999\%$ and $CH_3I > 99.99\%$. A more detailed description of the experimental procedure can be found elsewhere (Refs. [11] and [12]).

The ARAS technique used to observe Si-atom absorption at the Si-triplet $[4s\,^3P_2{}^* \leftarrow 3p_2\,^3P_2]$ at $\lambda = 251.6$ nm consists of a pulsed Si-hollow cathode lamp, the shock tube absorption path, which is located 15 mm ahead of the end plate, a monochromator (0.25 m Jarrell Ash), and a photomultiplier (Burle IP28). Perpendicular to the Si-detection system, a second ARAS diagnostic system is arranged for simultaneously monitoring H atoms. H atoms were detected at Lyman alpha $\lambda = 121.6$ nm. The system consists of a microwave excited discharge lamp, a 0.5 m McPherson VUV monochromator, and a solar blind photomultiplier (Hamamatzu Typ R1459). The microwave lamp was operated with a flowing gas mixture of 0.1% H_2 in He maintained at a constant pressure of 6 mbar and a microwave power of about 50 W. The spectral resolutions are 0.5 nm for the Si- and 0.6 nm for the H-diagnostic systems.

The spectral shape of both the Si- and H-atom resonance lines are not known precisely due to self absorption and self reversal in the light sources. Therefore, series of shock wave calibration experiments have been performed to relate the measured absorptions to the appropriate concentrations. The Si-atom calibration is based on the well known high-temperature dissociation of 0.05 to 2.0 ppm SiH_4 highly diluted in argon, see Mick *et al.* [13]. H atom calibration was realized by H atom measurements during the thermal decomposition of 2 ppm $N_2O/200$ ppm H_2/Ar mixtures at $1300\,K \le T \le 1900\,K$. The signals were compared with computer simulations, see Roth and Just [14, 15], and Masten *et al.* [16]. The relation between measured absorption and corresponding concentration can be expressed by the modified Lambert–Beer equation:

$$A_{\lambda,X} = 1 - \exp\left(-\left(l \times \frac{\sigma_{\lambda,X}}{cm^3}\right) \times \left(\frac{[X]}{cm^{-3}}\right)^n\right), \quad X = Si, H \qquad (1)$$

where l is the length of the absorption path, λ the wave length and n the concentration exponent. The individual calibration parameters were: $n_{Si} = 0.95$, $\sigma_{Si} = 4.0 \cdot 10^{-13}\,cm^2$; $n_H = 0.56$, $\sigma_H = 1.31 \cdot 10^{-8}\,cm^2$. Eq. (1) fits the calibration measurements for Si quite well in the concentration range between $2.0 \cdot 10^{11}$ and $4.0 \cdot 10^{12}$ atoms cm^{-3}, and for H between $3.0 \cdot 10^{11}$ and $1.0 \cdot 10^{13}$ atoms cm^{-3}. The uncertainties of Eq. (1) are about 15% for each species.

Results and discussion

In a first experimental series Si atom concentration profiles were measured behind reflected shock waves in mixtures containing SiH_4 or Si_2H_6 and a large excess of CH_4 highly diluted in argon. The detailed experimental conditions of all experiments of this study are listed in Table 1. Fig. 1 shows an example for both an undisturbed Si absorption profile of a shock heated SiH_4/argon mixture and its perturbation by addition of 200 ppm CH_4 at three different temperatures. Time $t = 0$ is fixed to the shock heat-up which leads to an almost instantaneous formation of Si atoms indicated by the absorption step from 0 to about 90%. With additon of CH_4 a signal decrease was measured after the

Table 1. Experimental conditions.

Test gas mixture in Ar	T [K]	p [bar]
0.25–1.0 ppm Si_2H_6/25–1000 ppm CH_4	1550 – 1970	1.5 ± 0.15
0.5–1.0 ppm SiH_4/200–500 ppm CH_4	1740 – 2130	0.6 – 1.4
0.5–2 ppm Si_2H_6/20 ppm CH_3Cl	1580 – 2320	1.4 ± 0.1
0.25–0.5 ppm SiH_4/2.5–5.0 ppm CH_3Cl	1850 – 2600	1.25 ± 0.1
0.25 ppm Si_2H_6/5.0 ppm CH_3I	1550 – 2050	1.4 ± 0.7
0.5–1.0 ppm SiH_4/5.0–50 ppm CH_3I	1790 – 2580	1.3 ± 0.15

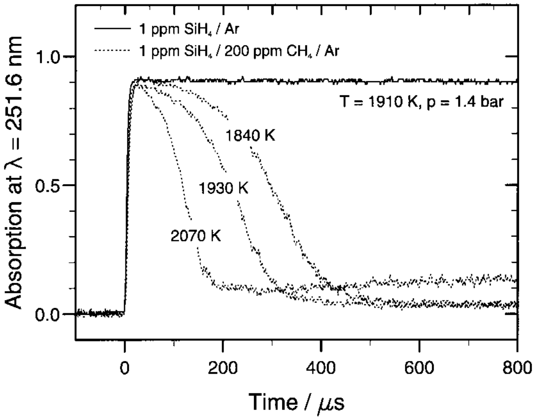

Fig. 1. Absorption at $\lambda = 251.6$ nm behind reflected shock waves in a SiH_4/Argon mixture without and with the addition of CH_4 at three different experimental temperatures.

maximum was reached and the decay became faster with increasing temperature. The *s*-formed shape of the profiles indicated an induction time for the consumption of Si atoms which is not explainable either by the uncertainty or lower sensitivity of the Si calibration relation at higher or lower absorption ranges. It signalizes that not CH_4 but a secondary reaction seems to be responsible for the consumption of Si atoms.

According to simulation calculations using the established GRI mechanism [17], CH_4 decomposes slowly and forms CH_3 as a major product within our temperature and pressure ranges. Therefore, a second series of experiments was performed in which the fast decomposition of either $CH_3Cl \rightarrow CH_3 + Cl$ (R20) [18] or $CH_3I \rightarrow CH_3 + I$ (R29) [19–21] were used as fast CH_3 sources. The main difference between the previous experiments was, that only a few ppm of CH_3Cl or CH_3I, i.e. almost two orders of magnitudes less than CH_4, were sufficient to reach a similar Si signal decay compared to the first experimental series. The measurements showed a strong dependence on the added CH_3Cl and CH_3I concentrations but no dependence on the experimental temperature. The apparent induction time found in the first series has disappeared, too. Fig. 2 shows measured Si absorption profiles when 5 ppm CH_3Cl and 10 ppm CH_3I were added to a 0.5 ppm SiH_4/Ar mixture. After a fast increase of the absorption within 20 μs caused by the fast formation of Si atoms, the signal tends to decrease over the next 300 μs. The ratios between the Si precursor concentrations (SiH_4, Si_2H_6) and the perturbing CH_3 source gas concentrations (CH_3Cl and CH_3I) of all investigated gas mixtures were kept at least at 1 : 10 and above. Calculations using the GRI mechanism showed that for almost all our experiments the amount of CH_3 could be treated in a first approximation to be constant within the period of the fast signal decay ($T = 1700$ K: 15% loss in $t = 1$ ms, $T = 2500$ K: 20% loss in $t = 0.2$ ms).

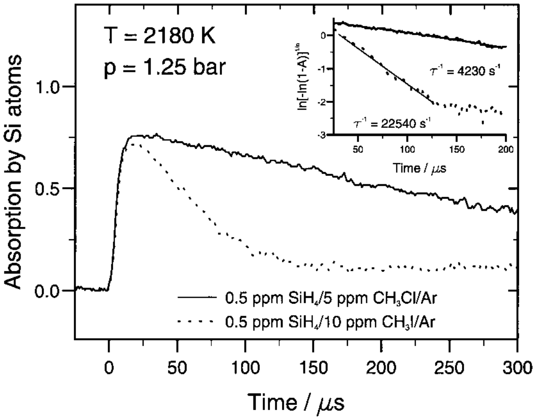

Fig. 2. Example of two absorption profiles by Si atoms which are measured in a SiH_4/Ar mixture with a few ppm CH_3I and CH_3Cl added. Insert: first-order plots of both absorption signals.

This justifies a pseudo-first-order analysis as a first step to determine a rate coefficient k_2^{1st} for the reaction of Si atoms with CH_3.

$$Si + CH_3 \overset{k_2}{\rightleftharpoons} \text{products} \tag{R2}$$

All measured Si absorption profiles were transfered into first-order plots, where $\ln\left[(-\ln(1-A_{Si}))^{(1/n)}\right]$ is plotted against the reaction time. The resulting curves of the measurements of Fig. 2 are presented in the upper right corner. Their slope is equal to the inverse time constant τ^{-1}:

$$\tau^{-1} = -\frac{d}{dt}\ln\left[(-\ln(1-A_{Si}))^{(1/n)}\right], \tag{2}$$

where A_{Si} is the Si-atom absorption. Rate coefficients k_2^{1st} of reaction (R2) can directly be determined from the time constants τ^{-1}.

$$k_2^{1st} = \frac{\tau^{-1}}{[CH_3]_0} \tag{3}$$

with $[CH_3]_0$ being the initial CH_3 concentration of a 100% conversion from CH_3I and CH_3Cl, respectiveley. The individual results are shown as open circles in Fig. 3. The rate coefficients are temperature-independent within our investigated temperature range. The mean-value is $k_2^{1st} = 2.19 \pm 0.7 \cdot 10^{14}\ cm^3\ mol^{-1}\ s^{-1}$ where the uncertainty is given at 1σ-level.

Possible reaction pathways are determined by comparing reaction enthalpies calculated using the thermodynamic data of the CHEMKIN database [22] containing ab-initio calculations from Allendorf and Melius [23] for

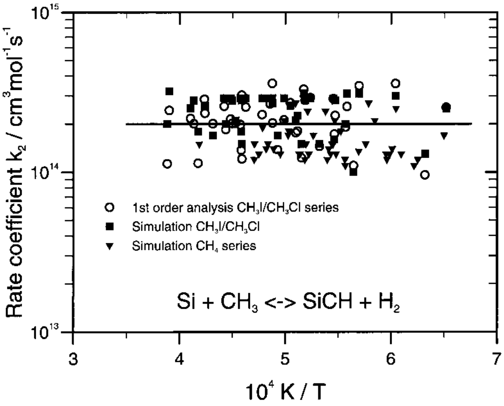

Fig. 3. Arrhenius plot of the rate coefficient k_2^{1st} and k_2^{sim} for the reaction of Si atoms with CH_3.

the Si-C-H system although they admit very high uncertainties in the data for molecules like HSiC and SiCH.

$$Si + CH_3 \overset{k_{2a}}{\rightleftharpoons} SiCH + H_2 \qquad \Delta H^0_{298} = -75.8\,\text{kJ/mol} \qquad \text{(R2a)}$$

$$\overset{k_{2b}}{\rightleftharpoons} SiCH_2 + H \qquad \Delta H^0_{298} = -68.2\,\text{kJ/mol} \qquad \text{(R2b)}$$

$$\overset{k_{2c}}{\rightleftharpoons} SiH + CH_2 \qquad \Delta H^0_{298} = 174.5\,\text{kJ/mol} \qquad \text{(R2c)}$$

$$\overset{k_{2d}}{\rightleftharpoons} HSiC + H_2 \qquad \Delta H^0_{298} = 177.3\,\text{kJ/mol} \qquad \text{(R2d)}$$

Reaction pathways (R2a) and (R2b) are exothermic; reaction enthalpies of other product channels than (R2c) and (R2d) are much more endothermic and are not listed here. (R2a) and (R2b) are the favoured channels because of the temperature independent k_2^{1st} that we obtained. To distinguish the pathway of reaction (R2), simultaneous H atom concentration measurements were performed. An example is presented in Fig. 4, where both, Si and H profiles are measured simultaneously in a $SiH_4/CH_3Cl/Ar$ mixture. For comparison, H profiles measured in a 2.5 ppm CH_3Cl/Ar mixture (dots) and in a 0.25 ppm SiH_4/Ar mixture (triangles) are also shown. The H concentration shows an explicitly slower increase compared to the Si concentration decay thereby indicating the dominance of channel (R2a) compared to the H producing channel (R2b).

It was observed that at higher temperatures and higher concentrations of CH_3Cl and CH_3I the Si-signal decay did not end at zero concentration levels as can be seen in Fig. 5. The signal continues after a fast decrease with a second slower increase which follows then again by a slow signal decay within our experimental measurement time. This behaviour was measured at

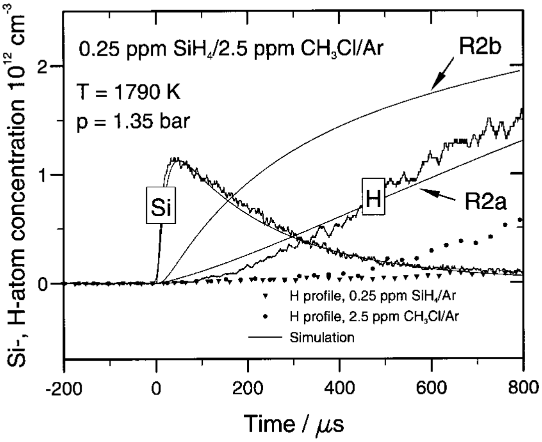

Fig. 4. Simultaneously measured Si- and H-atom concentration profiles compared with simulation results using reaction channel (R2a) and (R2b). H concentrations measured in CH_3Cl/Ar (dots) and SiH_4/Ar (triangles) mixtures are included.

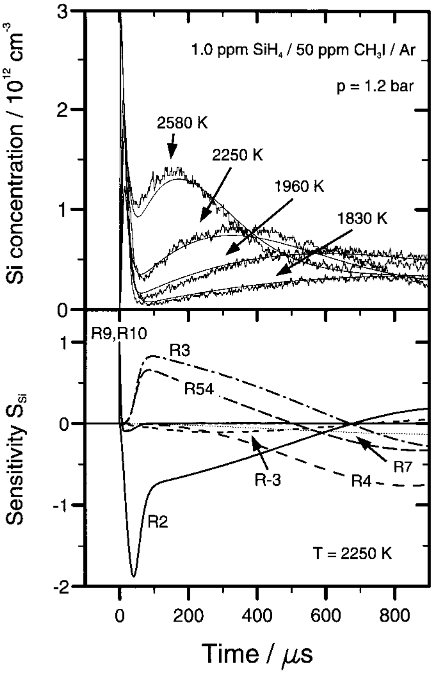

Fig. 5. Upper part: Si concentrations measured at four increasing temperatures in a 1 ppm SiH_4/50 ppm CH_4I/Ar mixture. Results of calculations obtained with the reaction mechanism of Table 2 are included. Lower part: Appropriate sensitivity analysis for Si atoms of the experiments at $T = 2250$ K with R54: $CH_3 + CH_3(+M) \rightleftharpoons C_2H_6(+M)$.

Table 2. Simplified reaction mechanism, $k_i = A \times T^n \times \exp(-T_A/T)$ $\mathrm{cm^3\,mol^{-1}\,s^{-1}}$.

	Reaction	Rate Coefficient			Ref.
		A	n	T_A	
1	$Si + CH_4 \rightleftharpoons SiCH_2 + H_2$	$< 1.0 \cdot 10^{12}$			t.s.
2	$Si + CH_3 \rightleftharpoons$ products	$2.0 \cdot 10^{14}$			t.s.
3	$SiCH + H \rightarrow Si + CH_2$	$7.0 \cdot 10^{12}$	1.15	11 930	as.
−3	$Si + CH_2 \rightarrow SiCH + H$	$1.0 \cdot 10^{15}$			as.
4	$Si + C_2H_2 \rightleftharpoons SiC_2 + H_2$	$1.2 \cdot 10^{14}$			[7]
5	$Si + C_2H_4 \rightleftharpoons SiH_2 + C_2H_2$	$5.3 \cdot 10^{13}$			[6]
6	$SiCH + CH_3 \rightleftharpoons Si + C_2H_4$	$< 4.0 \cdot 10^{12}$			t.s.
7	$Si + CH_2 \rightleftharpoons SiC + H_2$	$2.0 \cdot 10^{14}$			as.
8	$Si_2H_6 \rightleftharpoons SiH_4 + SiH_2$	$5.2 \cdot 10^{10}$		16 850	[24]
9	$SiH_4 \rightleftharpoons SiH_2 + H_2$	$1.9 \cdot 10^{10}$		22 550	[13]
10	$SiH_2 + Ar \rightleftharpoons Si + H_2 + Ar$	$9.1 \cdot 10^{13}$		15 100	[13]
11	$CH_3Cl \rightleftharpoons CH_3 + Cl$	$1.4 \cdot 10^{15}$		41 373	[18]
12	$Cl + CH_3Cl \rightleftharpoons HCl + CH_2Cl$	$3.4 \cdot 10^{13}$		1425	[18]
13	$CH_3 + Cl \rightleftharpoons CH_2 + HCl$	$2.2 \cdot 10^{13}$		4152	[25]
14	$HCl + Ar \rightleftharpoons H + Cl + Ar$	$9.0 \cdot 10^{13}$		44 010	[26]
15	$H + HCl \rightleftharpoons Cl + H_2$	$1.3 \cdot 10^{13}$		1700	[26,27]
16	$HCl + Cl \rightleftharpoons H + Cl_2$	$7.4 \cdot 10^{13}$		23 810	[28,29]
17	$H_2 + Ar \rightleftharpoons H + H + Ar$	$2.2 \cdot 10^{14}$		48 300	[30]
18	$Cl_2 + Ar \rightleftharpoons Cl + Cl + Ar$	$4.0 \cdot 10^{13}$		23 840	[28,31]
19	$CH_3I + Ar \rightarrow CH_3 + I + Ar$	$2.3 \cdot 10^{15}$		19 845	[21,19]
20	$H_2 + I \rightarrow HI + H$	$1.7 \cdot 10^{14}$		16 940	[28]
21	$HI + I \rightarrow H + I_2$	$8.0 \cdot 10^{14}$		18 700	[28]
22–69	GRI – Mechanism 3.0				[17]

temperatures above $T = 2000$ K in mixtures containing more than a tenfold excess of CH_3I and CH_3Cl, respectively. It was also observed in mixtures with an excess of CH_4. The beginning of this tendency at the lower temperature limit can be seen in Fig. 1 at $T = 2070$ K. In case of CH_3Cl the second increase was less pronounced. After the fast Si decay the signal ends in an almost steady state and was then followed by a slow decrease. Experiments with only $CH_4/CH_3Cl/CH_3I$/argon mixtures were performed at similar conditions to verify if secondary species, formed during the decomposition process, absorb at $\lambda = 251.6$ nm. No absorption was measured in these experiments.

Based on all these observations a reaction mechanism is proposed (see Table 2) containing the GRI mechanism [17], but without oxygen and nitrogen containing species and reactions, and the decomposition mechanisms of SiH_4 and Si_2H_6 [13, 24]. Dissociation reactions for CH_3I [21] and CH_3Cl [18] are added as well as reactions with Cl and HCl for completition. A reaction

$Si + CH_4 \rightleftharpoons SiCH_2 + H_2$ (R1a) was included based on thermodynamic considerations:

$$Si + CH_4 \overset{k_{1a}}{\rightleftharpoons} SiCH_2 + H_2 \qquad \Delta H^0_{298} = -65.5\,\text{kJ/mol} \tag{R1a}$$

$$\overset{k_{1b}}{\rightleftharpoons} SiH + CH_3 \qquad \Delta H^0_{298} = 153.6\,\text{kJ/mol} \tag{R1b}$$

$$\overset{k_{1c}}{\rightleftharpoons} SiCH_3 + H \qquad \Delta H^0_{298} = 154.1\,\text{kJ/mol} \tag{R1c}$$

$$\overset{k_{1d}}{\rightleftharpoons} SiH_2 + CH_2 \qquad \Delta H^0_{298} = 282.4\,\text{kJ/mol} \tag{R1d}$$

Reaction (R2a) as well as reactions $Si + C_2H_2$ and $Si + C_2H_4$ suggested by Basu and Husain [6, 7] were added using energetically favoured product channels.

The Si decay of all CH_3I and CH_3Cl experiments as well as all experiments with CH_4 could be simulated with this mechanism. This confirms on one hand the assumption of a slow reaction of Si with CH_4 compared to the fast one of Si with CH_3. On the other hand it validates the GRI mechanism for the CH_4 decomposition and the CH_3 formation, respectiveley. The resulting k_2^{sim} are also included in Fig. 3 and a mean rate coefficient k^2 containing all k_2^{1st} and k_2^{sim} for the reaction

$$Si + CH_3 \overset{k_2}{\rightleftharpoons} \text{products} \tag{R2}$$

can be given as:

$$k_2 = 2.00 \pm 0.69 \cdot 10^{14}\,\text{cm}^3\,\text{mol}^{-1}\,\text{s}^{-1}\,.$$

Fig. 6 shows the good agreement between a calculated and measured Si profile in a shock heated $SiH_4/CH_4/Ar$ mixture. The result of a sensitivity analysis with respect to Si is presented in the lower part of this figure. The sensitivity coefficients S_{Si} are plotted over time and the strong influence of reaction (R2) compared to (R1) becomes obvious. A maximum value can be given for the reaction of Si with CH_4 to be $k_1 < 1 \cdot 10^{12}\,\text{cm}^3\,\text{mol}^{-1}\,\text{s}^{-1}$ which is the highest value up to which the Si profiles can not be corrected by variations of k_2 within the error limit. Simulated Si and H atom profiles are shown together with the experimental results in Fig. 4. The calculations were performed by switching on either reaction (R2a) or (R2b). Whichever channel is switched on, it is seen that the result for the Si concentration matches the experimental value almost perfectly, whereas the H concentration is very much overpredicted with the (R2b) channel on. On the other hand the profile fits better with the experimental curve, despite slight uncertainties, when the channel (R2a) alone is allowed to proceed. This again reinforces that (R2a) is the dominant channel in the production of Si. Therefore, an upper limit can be given for the branching ratio $k_{2b}/k_{2a} < 0.17$ by considering the uncertainties of the H-ARAS calibration.

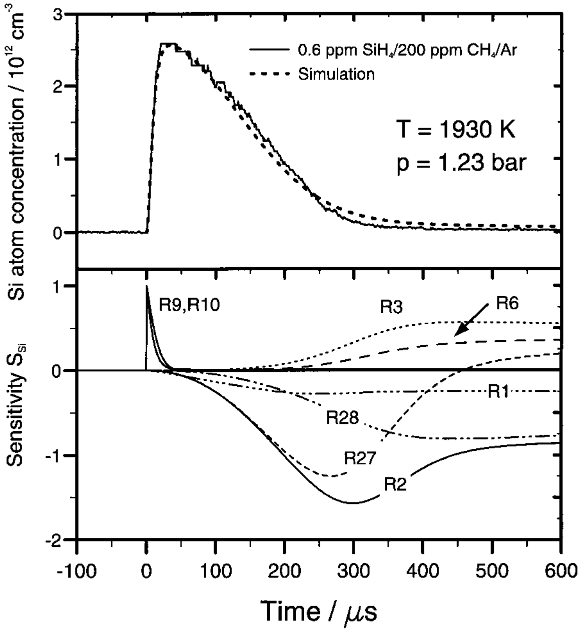

Fig. 6. Upper part: Comparison of a measured and calculated Si concentration profile in a $SiH_4/CH_4/Ar$ mixture. Lower part: Sensitivity analysis for Si atoms showing the strong influence of reaction $Si + CH_3$ (R2). R27: $CH_4(+M) \rightleftharpoons CH_3 + H(+M)$, R28: $H + CH_4 \rightleftharpoons CH_3 + H_2$.

The second formation of Si atoms (see. Fig. 5) can be either caused by decomposition or bimolecular reactions of radicals formed by reaction (R2). These possibilities were tried out and it was found that reactions $SiCH + Ar \rightleftharpoons SiC + H + Ar$, $\Delta H^0_{298} = 417.2$ kJ/mol, $SiC + H \rightleftharpoons Si + CH$, $\Delta H^0_{298} = 524.3$ kJ/mol, and $SiC + Ar \rightleftharpoons Si + C + Ar$, $\Delta H^0_{298} = 447.7$ kJ/mol could not explain the measured profiles.

The best fit of all profiles was achieved by including the very simple overall reaction of SiCH with H forming Si and CH_2.

$$SiCH + H \xrightarrow{k_3} Si + CH_2 \qquad \Delta H^0_{298} = 99.2\ \text{kJ/mol} \qquad \text{(R3)}$$

$$k_3 = 7.0 \cdot 10^{12} T^{1.15} \exp(-11\,930\ \text{K}/T)\ \text{cm}^3\,\text{mol}^{-1}\,\text{s}^{-1}$$

The backward reaction (−R3) is also considered and is set to a maximum value of $k_{-3} = 1.0 \cdot 10^{15}$ cm^3 mol^{-1} s^{-1}, but has no influence on the presented results. A reaction $Si + CH_2 \rightarrow SiC + H_2$ (R7) is included with a rate coefficient similar to k_2 but this had a negligible influence. The reaction $SiCH + CH_3 \rightarrow Si + C_2H_4$ (R6) is included with a maximum rate coefficient of $4.0 \cdot 10^{12}$ cm^3 mol^{-1} s^{-1}. Results at four different temperatures are shown in Fig. 5 which are achieved by k variations of the reactions (R2), (R3), and (R6) within their error limits. Calculations with the above estimated maximum branching ratio for (R2a) and (R2b) are found to result in incorrect predictions for the simulated Si profiles when compared to actual measurements at higher temperatures and higher CH_3 concentrations. The additional H atoms formed by the fast reaction (R2b) varies the Si concentration in its shape and absolute value, which can not be balanced by varying the value of k_3. A reduction of the upper limit of the branching ratio k_{2b}/k_{2a} from 0.17 to 0.10 leads to calculated profiles which fall within the measurement uncertainties. The lower part of Fig. 5 shows the eight most sensitive reactions for the experiment at $T = 2250\,K$. Small uncertainties of the H concentrations have an influence on the calculated Si concentration. In case of those experiments with a high excess of CH_3Cl such uncertainties are conceivable due to reactions between Cl and HCl with other species which are not known. The slightly different Si profile shapes in case of CH_3Cl, where the second Si increase is less strong, could easily be predicted with the mechanism by slight variations of the H concentrations by a few percent.

Conclusions

The reaction of Si with CH_3 is part of the gas phase chemistry of SiC synthesis. The kinetics of this reaction was studied in a shock tube behind reflected waves at temperatures $1500 \leq T \leq 2650\,K$ and pressures $0.6 < p < 1.4$ bar using different CH_3 and CH_4 sources to perturb a constant Si concentration obtained from the thermal decomposition of SiH_4 or Si_2H_6. The measured Si absorption decay was evaluated by a pseudo-first-order analysis. H atom concentrations were measured simultaneously to determine the reaction pathway. A reaction mechanism containing the GRI mechanism is proposed that could predict all measured Si- and H-atom concentration profiles. A rate coefficient is given for the reaction $Si + CH_3 \overset{k_2}{\rightleftharpoons}$ products (R2) which was found to be much faster than the rate coefficient for the reaction of $Si + CH_4$ for which an upper limit could be given. The product channel $Si + CH_3 \rightleftharpoons SiCH + H_2$ (R2a) was found to be dominant over the channel $Si + CH_3 \rightleftharpoons SiCH_2 + H$ (R2b) and an upper limit for the branching ratio $k_{2b}/k_{2a} < 0.1$ could be deduced.

Acknowledgement

The authors thank Mrs. N. Schlösser and Mr. L. Köppers for their help in performing and evaluating the experiments. The financial support of the Deutsche Forschungsgemeinschaft is gratefully acknowledged.

References

1. J. E. Bailey, M. Bohnet and J. Brinder, *Ullmann's Encyclopedia of Industrial Chemistry,* Vol. 6E, Wiley, John & Son, Inc., New York, USA (1999).
2. M. S. Wooldridge, Gas-phase combustion synthesis of particles, Prog. Energy Combust. Sci. **24** (1998) 63.
3. S. E. Pratsinis, Flame aerosol synthesis of ceramic powders, Prog. Energy Combust. Sci. **24** (1998) 197.
4. Y. Tamou, T. Yoshida and K. Akashi, The synthesis of ultrafine silicon carbide in a hybrid plasma, J. Jpn. Inst. Met. **51** (1987) 737.
5. J. Y. Guo, F. Gitzhofer and M. I. Boulos, Effects of process parameters on ultrafine SiC synthesis using induction plasmas, Plasma Chem. Plasma Process. **17** (1997) 219.
6. S. C. Basu and D. Husain, Absolute rate data for the reaction of ground state atomic silicon, $\mathrm{Si}\,(3^3P_J)$, with olefins determined by time-resolved atomic resonance absorption spectroscopy, Z. Phys. Chem. (Munich) **158** (1988) 1.
7. S. C. Basu and D. Husain, Measurement of absolute rate data for the reactions of ground state atomic silicon $\mathrm{Si}\,(3^3P_j)$ with acetylenes by time-resolved atomic resonance absorption spectroscopy, J. Photochem. Photobiol. **42** (1988) 1367.
8. D. Husain and P. E. Norris, Kinetic study of ground state silicon atoms, $\mathrm{Si}[3p^2(^3P_J)]$, by atomic absorption spectroscopy, J. Chem. Soc., Faraday Trans. 2 **74** (1978) 93.
9. A. Kunz and P. Roth, Shock tube study of the reaction of Si atoms with $SiCl_4$, Ber. Bunsenges. Phys. Chem. **102** (1998) 1492.
10. D. Husain and P. E. Norris, Kinetic study of reactions of ground state silicon atoms, $\mathrm{Si}[3p^2(^3P_J)]$, by atomic absorption spectroscopy, J. Chem. Soc., Faraday Trans. 2 **74** (1978) 106.
11. K. Thielen and P. Roth, Resonance absorption measurements of N and O atoms in high temperature NO dissociation and formation kinetics. Symp. (Int.) Comb. [Proc.] **20** (1984) 685.
12. D. Woiki and P. Roth, A shock tube study on the thermal decomposition of CS_2 based on $S(^3P)$ and $S(^1D)$ concentration measurements, Shock Waves **4** (1994) 95.
13. H. J. Mick, V. N. Smirnov and P. Roth, ARAS measurements on the thermal decomposition of silane, Ber. Bunsenges. Phys. Chem. **97**(6) (1993) 793.
14. P. Roth and Th. Just, Messungen zur Hochtemperaturpyrolyse von Äthan. Ber. Bunsenges. Phys. Chem. **83** (1979) 577.
15. Th. Just, *Atomic Resonance Absorption Spectrometry in Shock Tubes,* Marcel Dekker Inc., New York and Basel (1981).
16. D. A. Masten, R. K. Hanson and C. T. Bowman, Shock tube study of the reaction $H + O_2 \rightarrow OH + O$ using OH laser absorption, J. Phys. Chem **94** (1990) 7119.
17. G. P. Smith, D. M. Golden, M. Frenklach, N. W. Moriary, B. Eiteneer, M. Goldenberg, C. T. Bowman, R. K. Hanson, S. Song, W. C. Gardiner Jr., V. V. Lissianki and Z. Qin, *GRI MECH 3.0,* University of California at Berkeley, Dep. Mech. Eng., http://www.me.berkeley.edu/gri_mech/ (2000).
18. K. P. Lim and J. V. Michael, The thermal decomposition of CH_3Cl using the Cl-atom absorption method and the bimolecular rate constant for $O + CH_3$ (1609–2002 K) with a pyrolysis photolysis-shock tube technique, J. Chem. Phys. **98**(5) (1993) 3919.
19. S. S. Kumaran, M. C. Su and I. V. Y. Michael, Thermal decomposition of CH_3I using I-atom absorption, Int. J. Chem Kinet. **29** (1997) 535.
20. D. F. Davidson, M. D. Di Rosa, E. J. Chang and R. K. Hanson, An improved determination of the 216.615 nm absorption coefficient for methyl radicals, J. Quant. Spectrosc., Radiat. Transfer **53** (1994) 581.

21. K. Takahashi, A. Inoue and T. Inomata, Direct measurements of rate coefficients for thermal decomposition of methyl halides using shock-tube ARAS technique, Proc. 20th Symp. on Shock Waves **II** (1995) 959.
22. R. J. Kee, F. M. Rupley and J. A. Miller, The chemkin thermodynamic data base, Sandia Report SAND87-8215B, Sandia National Laboratories, April (1994).
23. M. D. Allendorf and C. F. Melius, Theoretical study of the thermochemistry of molecules in the Si-C-H system, J. Phys. Chem **96** (1992) 428.
24. H. J. Mick, M. W. Markus, P. Roth and V. N. Smirnov, A shock tube study of the thermal decomposition of Si_2H_6 based on Si and SiH_2 measurements. Ber. Bunsenges. Phys. Chem. **99**(6) (1995) 880.
25. A. Goldbach, F. Temps and H. G. Wagner, Kinetics of the reactions of $CH_2(X^3B_1)$ with HCl and HBr. Ber. Bunsenges. Phys. Chem. **94** (1990) 141.
26. G. N. Schading and P. Roth, Thermal decomposition of HCl measured by ARAS and IR diode laser spectroscopy, Combust. Flame **99** (1994) 467.
27. T. C. Allison, G. C. Lynch, D. G. Truhlar and M. S. Gordon, An improved potential energy surface for the H_2Cl system and its use for calculations of rate coefficients and kinetic isotop effects, J. Phys. Chem. **100** (1996) 13 575.
28. D. L. Baulch, J. Duxbury, S. J. Grant and D. C. Montague, Evaluated kinetic data for high temperature reactions. Vol. 4, Homogeneous gas phase reactions of halogen- and cyanide-containing species, J. Phys. Chem. Ref. Data 10, Suppl. 1 (1981).
29. B. C. Garrett and D. G. Truhlar, Generalized transition state theory. Canonical variational calculations using the bond energy-bond order method for bimolecular reactions of combustion products, J. Am. Chem. Soc. **101** (1976) 5207.
30. D. L. Baulch, D. D. Drysdale, D. G. Horne and A. C. Lloyd, Homogeneous gas phase reactions of the H_2-O_2 system, Vol. 1 of *Evaluated Kinetic Data for High Temperature Reactions*, Butterworth, London, 1. ed. (1972).
31. A. C. Lloyd, A critical review of the kinetics of the dissociation-recombination reactions of fluorine and chlorine, Int. J. Chem. Kinet. **3** (1971) 39.